On the synthesis and potential benefit of Na-rich P-type layered oxides for high power Na-ion batteries

Ghassen Charrad, Justine Harmel, Romain Berthelot, Pierre-Louis Taberna, Patrice Simon, Patrick Rozier

On the synthesis and potential benefit of Na-rich P-type layered oxides for high power Na-ion batteries.

Ghassen Charrad[1,2,3], Justine Harmel [1,2], Romain Berthelot[2,3], Pierre-Louis Taberna[1,2], Patrice Simon[1,2], Patrick Rozier[1,2]

[1] Université Toulouse III Paul Sabatier, CIRIMAT UMR CNRS 5085, 118 Route de Narbonne, Toulouse 31062, France

[2] Réseau sur le Stockage Electrochimique de l'Energie (RS2E), CNRS, Amiens, France

[3] ICGM, Université Montpellier, CNRS, ENSCM, Montpellier, France

Abstract

Layered oxides with the general composition Na_xMO_2 (M=transition metal) have attracted a lot of attention for their composition diversity and promising electrochemical performances as positive electrode for sodium-ion batteries. P-type compositions offer power capabilities owing to the fast diffusion of sodium cations but are plagued by limited specific capacities because of the nominal low amount of sodium in the structure. Therefore, sodium enriching of P-type structure is consequently of interest to propose electrode candidates combining high energy density and high power capabilities.

Herein co-precipitation syntheses of sodium-rich P-type $Na_xMn_{2/3}Ni_{1/3}O_2$ and $Na_xMn_{1/2}Ni_{1/2}O_2$ have been attempted and the synthesis mechanism carefully monitored by X-rays diffraction follow up in temperature. The optimization of the synthesis protocol led to stabilize only P3-type single-phases. The combination of several characterization techniques shows that the actual Na content is limited to x=0.8 far from targeted stoichiometry but still higher than conventionally reported for most of P3-type layered oxides.

The investigation of the electrochemical behavior of Na-rich P3-type compounds shows that they behave similarly to stable P2-type and O3-type homologue used as reference.

Consequently, efficiency of highly sodiated P3-type layered oxides as a way to combine high energy density and power capabilities is questioned while the interest in stabilizing Na-rich P2-type remains an open question.

Keywords: Na-ion battery; P-type cathode; soft chemistry synthesis;

1. Introduction

Lithium-ion batteries (LIBs) are today the dominant battery chemistry and lead the market segments ranging from power electronics to electric vehicles thanks to their high energy density. The fast development of the LIB technology questions the availability of metals needed for assembling LIB cells such as Li, Cu, and Co [1,2]. Recently, sodium-ion batteries (SIBs) have attracted considerable interest as the most promising alternative to LIBs [3] especially for future large-scale energy storage in light of low cost and large abundance of sodium resources [4]. Cathode materials being the key component that drives the energy density of this chemistry, many efforts have been devoted to explore and develop the most suitable positive electrode materials with large reversible capacity, fast sodium insertion/extraction and good cyclability [5]. Among the cathode candidates, layered alkali transition metal oxides Na_xMO_2 are the most promising for SIBs [6]. The structure of layered Na_xMO_2 is formed by the stacking of MO_2 layers (built with edge-sharing MO_6 octahedra) with sodium cation being intercalated between them. The stacking mode of the MO_2 layers leads to design octahedral (O) or prismatic (P) sites for the inserted Na cations and different sequences governs the number "n" of the layers needed to recover the periodicity. Delmas notation [7], consisting on a letter describing the Na surrounding followed by the number of MO_2 layers in a repetition unit is widely used to describe the different combinations. It is well admitted that the thermodynamically stable Na_xMO_2 structure type depends on the Na content with P3-, P2- then O3- type usually obtained when sodium content x increases respectively from 1/2, to 2/3 and 1. The relationship between structure type and sodium content is also supported by the fact that (electro-)chemical insertion/deinsertion of Na in O3-

type leads to the conversion to P3-type and in P2-type to the formation of a O2-type structure that has, in addition, never been obtained by direct synthesis.

Beside the Na content, the stacking sequence induces drastic differences of the sodium cation diffusion. In P-type stacking, sodium cations move directly through rectangular face shared by two adjacent prismatic sites, while the diffusion pathway involves intermediate and highly unfavorable tetrahedral sites in O-type structures.[8] The easier cationic diffusion in P-type layered oxides is beneficial to promote high power capabilities, but, unfortunately, is associated to compositions highly deficient in sodium. Indeed, mainly the compositions P3-$Na_{1/2}MO_2$ and P2-$Na_{2/3}MO_2$ are commonly reported, and induce, considering practical full cells without sodium reservoir, a capacity loss of 50 and 33 %, respectively, in comparison with stoichiometric O3-type Na_1MO_2.

Following that, stabilizing highly sodiated P-type compositions is an attractive approach to combine both high capacity and high power capabilities. Recently, post-synthesis sodium enrichment has been attempted on stable P2-$Na_{2/3}(Fe_{1/2}Mn_{1/2})O_2$ using either NaN_3, Na_3P or even metallic Na as reducing agents [9]. Although the corresponding electrochemical performance validate the approach, the chemical process is not easily scalable preventing its use for practical applications. Besides that, few reports show that high Na contents P-type structure can be directly stabilized by tuning the composition of the MO_2 layers, such as substituting Li to M [10] and/or by using alternative synthesis process such as soft chemistry[11,12]. However, despite announced Na-rich P-type structure and for some even stoichiometric P-Na_1MO_2 compounds, the actual Na content has been poorly investigated leading to some ambiguities in the reported capacity and no systematic study of the existence of a clear upper Na content limit is proposed.

With the aim of determining if stoichiometric P-Na_1MO_2 electrode materials can be stabilized by direct synthesis and what will be, if any, the advantage compare to stable Na deficient P2-

type or Na stoichiometric O3-type, we investigated two compositions (y=1/3 and y=1/2) in the $Na_x[Mn_{1-y}Ni_y]O_2$ system. These compositions are selected because the electrochemical behavior of thermodynamically stable P2-$Na_{\underline{2/3}}Mn_{2/3}Ni_{1/3}O_2$ and O3-$Na_1Mn_{1/2}Ni_{1/2}O_2$ analogs, known for years, is fully elucidated and so that these compounds can serve as reference.

Instead of conventional solid state synthesis process operating at high temperature, we aim to favor the fast diffusion of cationic species and lower the synthesis temperature to allow the obtaining of metastable phases. Consequently, we selected a two-step process enlisting first the co-precipitation of transition metal precursors. A benchmark of different transition metal and sodium precursors allowed to select a fully-hydroxide route further optimized to obtain high Na content P3-type compounds. The chemical compositions were carefully determined by combining chemical analysis, structural refinement and electrochemical sodiation, leading to show a maximal Na content approaching $x = 0.8$ far from targeted stoichiometric x=1 value. The investigation of the electrochemical behavior clearly shows the as-prepared P3-$Na_{0.8}[Mn_{1-y}Ni_y]O_2$ (y=1/3 ; 1/2) compounds actually behave like the references P2-$Na_{2/3}Mn_{2/3}Ni_{1/3}O_2$ and O3-$Na_1Mn_{1/2}Ni_{1/2}O_2$, respectively, which clearly questions the interest of stoichiometric P-type layered compounds as a solution to target both high energy density and high power performances Na-ion batteries.

2. Experimental section

The synthesis of high Na content P-type layered materials is performed via a two steps process including the preparation of mixed transition metal precursors (carbonate and hydroxide) using a co-precipitation route, and the calcination of the mixture of these precursors with different Na sources.

For the synthesis of the carbonate precursor, stoichiometric amounts of $MnSO_4.H_2O$ (≥99% Aldrich) and $NiSO_4.7H_2O$ (99% Aldrich) are dissolved in deionized (DI) water. Separately a

solution of Na_2CO_3 (≥99.5% Aldrich) (2M) and NH_4OH (0.2M) in DI water is prepared. The latter is added dropwise under N_2 at 55°C while maintaining pH=6.5 and left stirring overnight at the same temperature for particles growth. The pH domain was chosen according to the E-pH diagrams for Mn-CO_3-H_2O and Ni-CO_3-H_2O at T=55°C [13]. The precipitate is washed and filtrated with DI H_2O then dried at 100°C to remove excess of water.

For the synthesis of hydroxide precursors, stoichiometric amounts of $MnSO_4.H_2O$ and $NiSO_4.7H_2O$ are dissolved in DI H_2O to obtain a 2M aqueous solution. $Mn,Ni(OH)_2$ are co-precipitated using a batch reactor with controlled atmosphere. A solution of NaOH (≥99.5% Aldrich) (1M) and NH_4OH (0.2M) is added dropwise at 55°C under N_2 while maintaining pH=11 [14-16]. The solution is left stirring overnight then filtrated and washed with water to remove the sulfate anions. The obtained product is dried at 100°C for 12h.

The mixed metal precursor is hand grinded and mixed for 5 minutes with the selected sodium source (Na_2CO_3 or NaOH) in a stoichiometric amount (for NaOH a 10%wt excess is used to compensate for the adsorbed H_2O as determined using TGA experiments). The mixtures are calcined in air in a muffle oven at different temperatures for 12h (heating ramp 2°C/min). The sample is cooled down following the inertia of the oven then quenched from 300°C in a desiccator and transferred in glove box to avoid any side reaction with moist air.

Reference compounds O3-$NaMn_{1/2}Ni_{1/2}O_2$ and P2- $Na_{2/3}Mn_{2/3}Ni_{1/3}O_2$ are synthesized in 1 g batches via conventional high-temperature solid-state reaction[17,18]. Stoichiometric amounts of Na_2CO_3 (≥99.5% Aldrich), NiO (99.99% Strem Chemicals) and Mn_2O_3 (≥99.9% Aldrich) are ball-milled at 1725 rpm for 30min in a stainless steel jar using SPEX- miller (8000M Mixer/Mill). The mixture is heated at 900°C for 10h under air in a muffle oven with a heating rate of 2°C/min. The samples are first cooled down following the inertia of the oven then quenched from 300°C in a desiccator and transferred in glove box to avoid any side reaction with moist air.

Powder X-ray diffraction (XRD) patterns were recorded using a Bruker D4 diffractometer or Bruker D8 Endeavor both using Cu Kα radiation (λ= 1.54 Å). Diffraction patterns over the range 2θ=10−100° were collected with a scanning speed of 0.02°/s. All XRD pattern analysis were carried out using the FullProf software package [19].The investigation of the chemical process is performed by XRD follow up in temperature carried out by pressing a homogenous mixture of precursors on an alumina disk and placed in HTK1200N high temperature chamber installed on the Bruker D8 diffractometer. The samples were heated up to 900°C with a heating rate of 30°C.min^{-1} and the XRD patterns were collected each 100°C in the [10° - 100°] 2θ angle range. The investigation of the structure evolution during electrochemical process was operated using *operando* XRD performed with a Swagelok type cell equipped with a beryllium window protected by an aluminum foil as current collector. The cell is cycled at C/30 (1 Na exchanged in 30h) and each scan covers a range of 2θ from 10° to 50° in a duration of 1h.

Field Emission Gun-Scanning Electron Microscopy (FEG-SEM) observations were carried out on a JEOL 7800F. The chemical composition of the samples was determined using Inductively Coupled Plasma Emission Spectroscopy (ICP-AES) using spectrometer Varian 720-ES Optical Emission Spectrometer.

All procedures described below (sample preparation, coin cell or Swagelok assembly) were performed in Ar-filled glovebox with water and oxygen levels below 1 ppm.

Pristine active material (80wt.%) and Carbon sp (20wt.%) were mixed by ball milling for 30 minutes (SPEX), recovered and stored in the glovebox to be used directly in Swagelok cells. A sodium metal foil pressed onto aluminum current collector was used as negative electrode and a separator of borosilicate sheets (Whatman, GF/D) was used. The mass loading of the cathode materials was fixed at ≈ 6 mg.cm^{-2}. The electrolyte used was 1M $NaPF_6$ in EC:DMC (1:1 v/v) with 5% fluoroethylene carbonate (FEC) additive.

For *operando* XRD, electrodes were made by casting a slurry of active material, carbon and PVDF binder (Kynar homopolymer) dispersed in N-methyl-2-pyrrolidone (Sigma-Aldrich, anhydrous, 99.5%) using an active material/carbon/binder mass ratio of 8:1:1 and an active material loading of 1.5 mg cm^{-2}. Disks (10 mm diameter) were punched out and dried at 120°C for 12 h under dynamic vacuum.

3. Results and discussion

3.1. Synthesis of Na-rich P-type layered oxides

The first part of our work is to optimize synthesis parameters to lower the reaction temperature with the aim of stabilizing Na-rich P-type structure. To suppress the well-known kinetic limitation associated to the low diffusion of cationic species in the solid state, the first step is to prepare transition metals precursors by co-precipitation protocols. Carbonate and hydroxide precursors have been prepared following the protocol described in the experimental section. XRD patterns of $Mn_{1/2}Ni_{1/2}CO_3$ and $Mn_{1/2}Ni_{1/2}(OH)_2$ (Figure SI 1, 2) confirm a single-phase product, with cell parameters, refined using the Le Bail method, in good agreement with a solid-solution behavior ($Mn_{1/2}Ni_{1/2}CO_3$, space group R-3c with a=4.794(9) Å and c= 15.617(9) Å and $Mn_{1/2}Ni_{1/2}(OH)_2$, space group P-3m1 with a=3.076(1) Å and c=4.612(3) Å). It is worth mentioning that the fine control of the pH along the whole hydroxide route process allows preventing the formation of usually obtained side products such as Mn_3O_4. After that, we monitored by an XRD follow up in temperature the synthesis process of the layered oxides during the calcination of the as-obtained transition metal precursors with either sodium carbonate or sodium hydroxide. As shown in Figure 1a, using carbonate precursors, the synthesis of the layered oxide is triggered around 400°C, as evidenced by the growing of a (00l) Bragg peak located at 2θ=15.64°, and really engaged at 500°C, as indicated by the identification of the full set of Bragg peaks characteristics of the

P3-type structure (space group *R*3*m*). In addition, side species Na_2CO_3 and NiO are observed indicating that the reaction is not complete. This mixture is maintained up to 800°C above which Bragg peaks characteristic of Na_2CO_3 vanish and fully disappear at 850°C. The increase of the temperature up to 900°C leads to the conversion from P3-type to P2-type structure (Space group $P6_3/mmc$[22]) while remaining NiO formed during the synthesis is still observed.

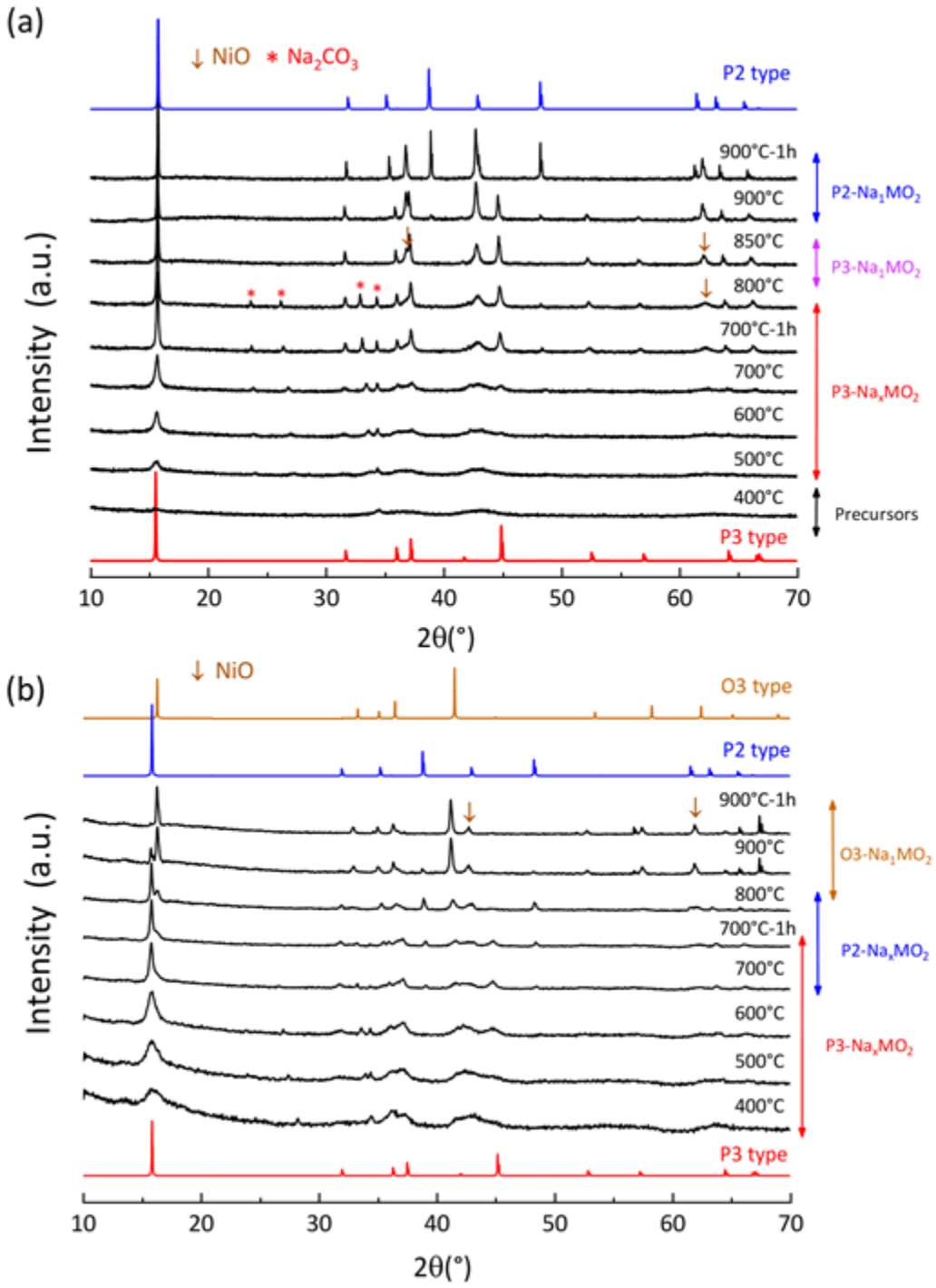

Figure 1 : XRD follow up in temperature of the mixture of (a) $Mn_{0.5}Ni_{0.5}CO_3$ + $NaCO_3$ and (b) $Mn_{0.5}Ni_{0.5}(OH)_2$ + NaOH heated up to 900°C with the existence domains of the different phases P3, P2 and O3-type.

Despite targeting Mn/Ni ratio equals to 1, the presence of NiO as impurities shows a limited solubility of Ni in $Na_xMn_{1-y}Ni_yO_2$ phase which is good agreement with reported data [23,24].

The presence in a wide range of temperature of unreacted Na_2CO_3 confirms that stoichiometric $Na_1Mn_{1-y}Ni_yO_2$ composition is not reached. The decreasing content of unreacted Na_2CO_3 with increase in temperature shows the progressive increase of the Na content (x) in the layered oxide Na_xMO_2 explaining the observed evolution of the structure type from P3-type (stable for low Na content) to P2-type (stable up to x=2/3). This conversion occurs at a temperature around 900°C where Na based reactants are also known to volatilize inducing a Na deficient mixture which may explain that the O3-type structure (stable polymorph for x=1) is not observed. While the use of mixed TM precursor allows avoiding the kinetic limitation associated with reaction between oxides, the presence of unreacted Na_2CO_3 until temperature as high as 800°C shows that Na_2CO_3 limits the kinetic and prevent completeness of the reaction.

To avoid this limitation, NaOH with a lower melting temperature (318 °C) than that of Na_2CO_3 (850 °C) is used and its reactivity with the carbonate transition metal precursor is tested. A mixture of $Mn_{1/2}Ni_{1/2}CO_3$ and NaOH is annealed for 12h at 700 °C, temperature selected, based on previous experiments, to allow obtaining homogeneous and well crystalized compounds while preventing structure conversion to stable polymorphs. The analysis of the XRD pattern of the as obtained sample (Figure SI 3) shows that it consists of a mixture between P3-type layered compound, NiO and still Na_2CO_3. While NaOH was used, the presence of Na_2CO_3, indicates that the CO_2 released during the decomposition of the $Mn_{1/2}Ni_{1/2}CO_3$ precursor reacts with Na source to form *in situ* Na_2CO_3 responsible for kinetic limitation.

Figure 1b illustrates a different story in case of a fully hydroxide route. The comparison of XRD patterns collected at different temperatures confirms that P-type compound is obtained at low temperature. The increase in temperature induces the progressive conversion from P3-type to P2-type structure in agreement with increase of Na content. Above 900°C, the

conversion to the stable and stoichiometric O3-$Na_1Mn_{1/2}Ni_{1/2}O_2$ compound is evidenced by the progressive growing of $(003)_{O3}$ Bragg peak (2θ=16.29°) at the expense of the $(003)_{P3}$ and $(002)_{P2}$ Bragg peaks. The progressive structure changes observed while increasing the reacting temperature confirms that the Na content depends on the temperature and that the use of hydroxide based reactants favors the progressive insertion of Na in the layered structure at a temperature low enough to prevent its volatilization. Based on these results, the fully hydroxide route is used for the synthesis of the layered oxide. $(Mn_{1-y}Ni_y)(OH)_2$ with y=1/3 and y=1/2 are mixed with NaOH and calcinated for 12h at different temperatures. The XRD patterns reported in Figure 2 shows that for both Mn/Ni ratio, at temperature as low as 500°C, a P3-type structure is obtained however mixed with Na_2CO_3. Although only hydroxide reactants were used, the presence of Na_2CO_3 could be explained by a side reaction, occurring during the cooling step, of unreacted Na precursor with ambient air and, unfortunately, evidences also that stoichiometric layered oxide is not obtained.

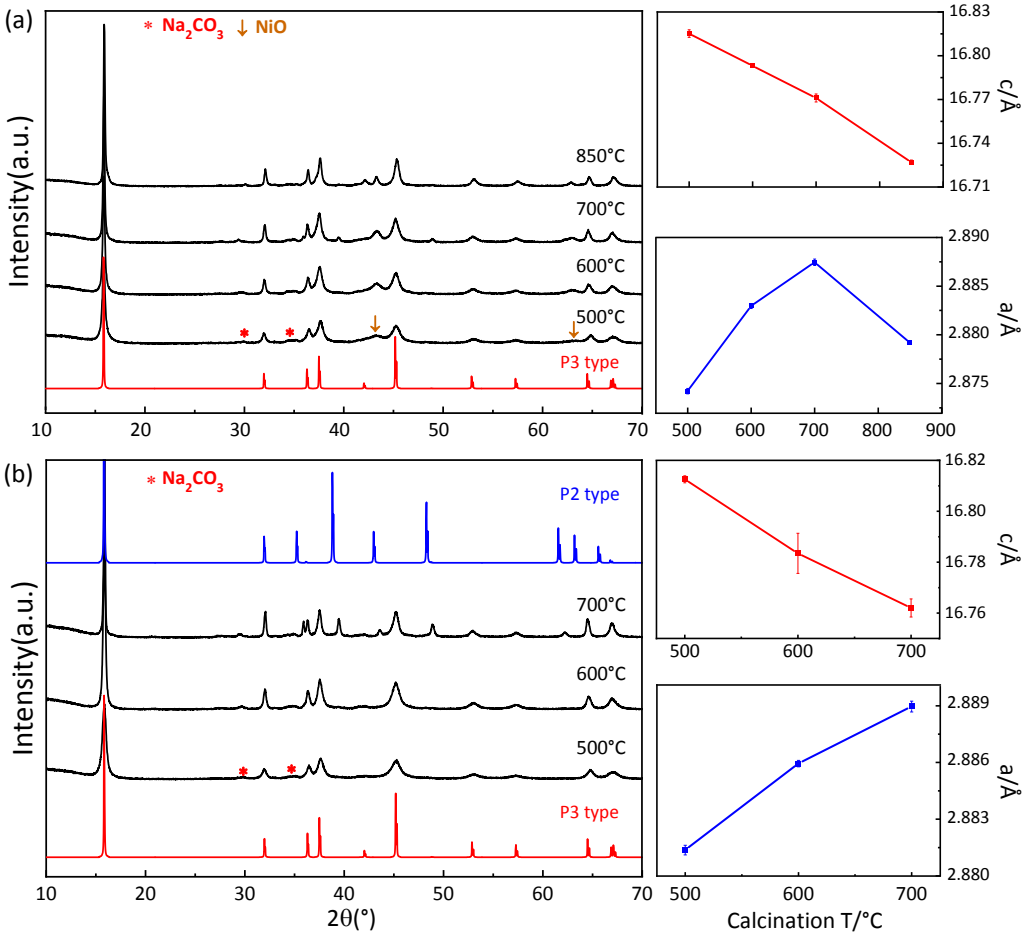

Figure 2 : Evolution with calcination temperature of XRD patterns and refined cell parameter for targeted P3-$Na_xMn_{1/2}Ni_{1/2}O_2$ and b) P3-$Na_xMn_{2/3}Ni_{1/3}O_2$ layered oxides.

Considering the composition $Na_xMn_{1/2}Ni_{1/2}O_2$ (Figure 2a), carbonate-free sample is achieved at 600 °C and the P3-type structure is maintained up to 850°C with evidences of NiO impurities in agreement with the already reported limited solubility of Ni in $Na_xMn_{1-y}Ni_yO_2$ [25]. For the composition $Na_xMn_{2/3}Ni_{1/3}O_2$ (Figure 2b), single phase P3-type structure is obtained up to 600°C above which the P2-stacking becomes visible. The lattice parameters of the P3-type phases obtained after calcination at different temperatures have been refined and their evolution is presented in Figure 2. It is well known that the c cell parameter is governed by the strength of the repulsive effect between oxygen from adjacent MO_2 layers which is screened by the Na^+ ions located in the interlayer space, whereas the a cell parameter characterizes the size of the MO_2 layers and is directly related to the nature and valence state of the transition metal ions. For the two compositions, the decrease of the c lattice parameter

with increase in calcination temperature can then be interpreted as an increase of the screening effect which is indirect evidence of the increase in the Na content. The slight increase of the a lattice parameter, while the MO_2 layer chemical composition does not change, shows progressive reduction of the transition metal (ionic radii increasing) and consequently agrees with a progressive sodium enrichment. Following that, reaching highest Na content of P3-type polymorph is a compromise between high calcination temperature to favor completeness of the reaction and low temperature to prevent structure conversion to stable polymorphs. In our case such optimized compounds correspond to P3-$Na_xMn_{1/2}Ni_{1/2}O_2$ calcinated at 850°C, and P3-$Na_xMn_{2/3}Ni_{1/3}O_2$ calcinated at 600°C which are selected for further characterizations. The most important characteristic being the actual sodium content, its accurate determination require combination of several techniques. Chemical analysis using ICP-AES characterization demonstrates that the experimental ratio Na/Ni/Mn are close to the nominal value of the designed samples (Table SI 1). The SEM images (Figure 3) shows that all samples are composed of agglomerates constituted with submicron particles, and EDS analysis confirms the homogeneous distribution of elements (Figure SI 4).

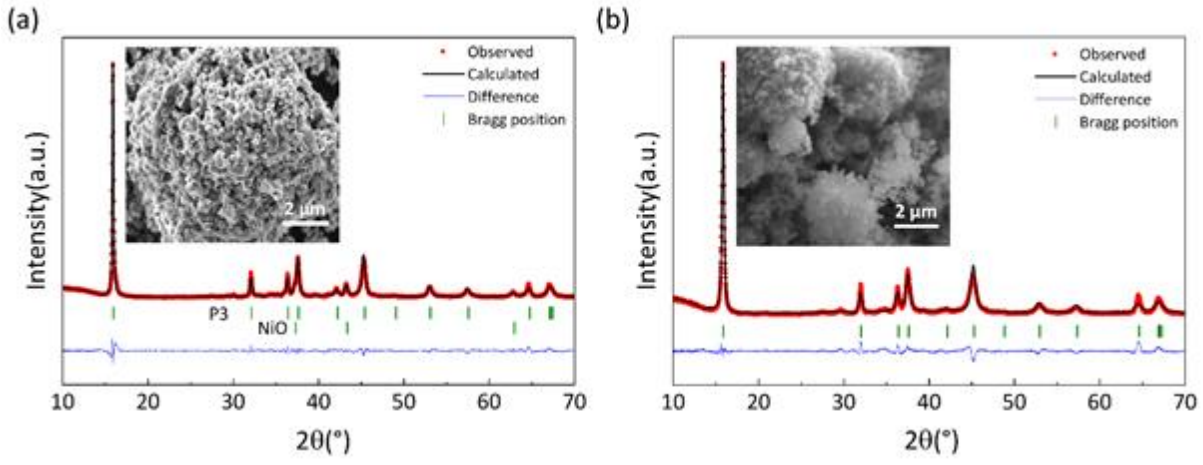

Figure 3 : Representation (limited to 2θ=70° for clarity) of Rietveld refinement results and SEM images of (a) P3-$Na_xMn_{1/2}Ni_{1/2}O_2$ calcinated at 850°C and (b) P3-$Na_xMn_{2/3}Ni_{1/3}O_2$ calcinated at 600°C.

Knowing that ICP analysis only gives average composition of the sample and that XRD is not sensitive enough to detect low amount of Na based side products, structure refinement is performed. The Rietveld refinement of the XRD patterns (Figure 3 and Table SI 2,3) confirms that P3-type structure is obtained for both samples and the presence of NiO impurity (5wt% as deduced from quantitative phase analysis) for P3-$Na_xMn_{1/2}Ni_{1/2}O_2$ sample. Despite the XRD patterns present broad peaks not well defined especially at high diffraction angle, thermal displacement and Na site occupancy have been refined leading to estimate sodium contents around 0.75. As these results remain qualitative, we also performed electrochemical sodiation in half-cells versus sodium metal through a galvanostatic discharge mode down to 1.5 V and compare the results with that obtained using stoichiometric O3-$Na_1Mn_{1/2}Ni_{1/2}O_2$ reference sample. While for the reference, the "discharge" capacity is equal to 0, for P3-type samples the discharge capacity is somehow equivalent and around 50 $mAh.g^{-1}$ (Figure SI 5). To estimate the corresponding Na content, two calculations are used. A first approach consider that the weighted sample corresponds to purely active material $Na_xMn_{1-y}Ni_yO_2$ with y value equals to nominal ones used for the synthesis. A second approach considers, in a more realistic way, that weighted sample is a mixture of active material and a dead mass corresponding to side species such as NiO and/or Na_2CO_3. The results compiled in Table SI-4 allow estimating that the Na content of all prepared samples is around 0.8.

To conclude on this part, the cross-combination of structural refinement and electrochemical analysis disagree the preliminary chemical analysis and estimates the amount of sodium around 0.8. The first objective of obtaining fully sodiated P3-type electrode is consequently not achieved despite optimized synthesis protocol. Thus, even if actual Na content is largely higher than the 0.5 Na content usually reported for stable P3-type structure [26,27], this questions the soft chemistry process as a viable methodological approach to stabilize stoichiometric P-type layered oxides.

3.2. Electrochemical behavior of Na-rich P-type layered oxides

Despite instead of targeted stoichiometric P3-Na_1MO_2 compounds Na-rich P3-$Na_{0.8}MO_2$ are obtained, we decided to investigate the electrochemical behavior of selected compounds and compare it with the one of corresponding reference samples P2-$Na_{2/3}Mn_{2/3}Ni_{1/3}O_2$ and O3-$Na_1Mn_{1/2}Ni_{1/2}O_2$ prepared using conventional solid state synthesis route (Figure SI 6). The electrochemical behavior of all samples were examined in a Na half-cell at current density of 0.1C in the [1.5-4.5 V] voltage range. The comparison of the galvanostatic charge/discharge voltage profiles collected along the first two cycles of the different samples (Figure 4) shows much more sloping profile for P3-type samples as compared to reference ones. This is in agreement with the presence of resistive unreacted species contributing also to the observed large polarization. In addition, as highlighted in the derivative dQ/dV plots (Figure SI 7), P3-type samples exhibit a high voltage plateau partially irreversible which can be attributed to the oxidation of unreacted Na_2CO_3 [28]. The voltage profiles of P3-$Na_{0.8}Mn_{2/3}Ni_{1/3}O_2$-600 and P3-$Na_{0.8}Mn_{1/2}Ni_{1/2}O_2$-850 (Figure 4) exhibit strong similarities with the references P2-$Na_{2/3}Mn_{2/3}Ni_{1/3}O_2$ and O3-$Na_1Mn_{1/2}Ni_{1/2}O_2$, respectively. These similarities are used to attribute, in light of the abundant literature reported for the reference phases, the different observed plateaus or pseudo-plateaus to Mn redox couples in the [1.5V – 2.5V] voltage range and to Ni redox couples in the [2.5V – 4.0V] one [23,29] while above 4.0V the reversible capacity can be attributed to anionic redox activation [30].

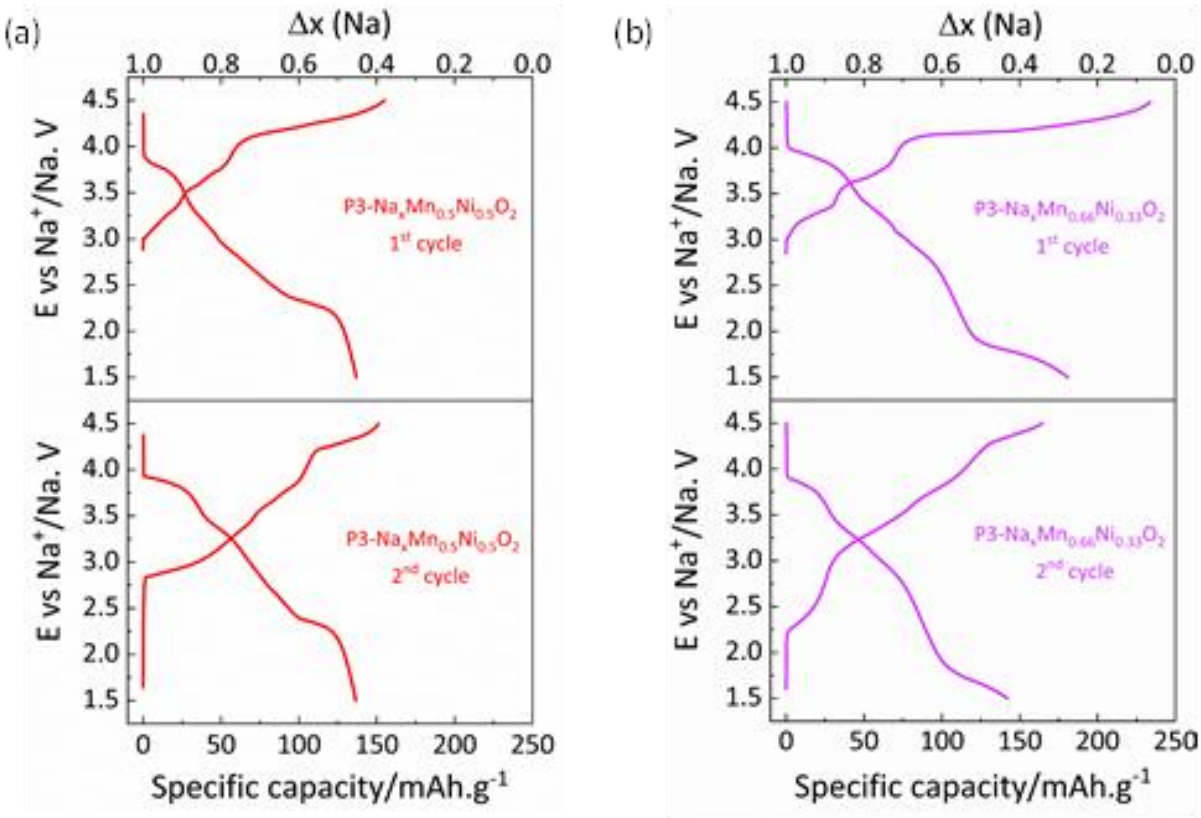

Figure 4 : Galvanostatic cycling curves during the first and second cycle between 1.5 V-4.5V at C/10 of (a) P3-$Na_xMn_{1/2}Ni_{1/2}O_2$ calcinated at 850°C and (b) P3-$Na_xMn_{2/3}Ni_{1/3}O_2$ calcinated at 600°C.

The similarity between the voltage profiles of P3-$Na_{0.8}Mn_{1/2}Ni_{1/2}O_2$-850 and reference O3-$Na_1Mn_{1/2}Ni_{1/2}O_2$ is somehow expected as it is well-known that the electrochemical extraction of Na from O3-type compounds leads to a biphasic process associated to the conversion from O3-type to P3-type [31]. This shows that using low temperature process, it is possible to synthesize directly one of the metastable compounds usually obtained using electrochemistry but also indicates the absence of advantage in preparing Na-rich P3-type structure which converts to stable O3-type homologue once full discharge is reached. The similarity of the voltage profile and more precisely the biphasic and solid solution domains between P3-$Na_{0.8}Mn_{2/3}Ni_{1/3}O_2$-600 and the reference P2-$Na_{2/3}Mn_{2/3}Ni_{1/3}O_2$ is more intriguing. In the light of conclusions showing that as already widely reported ([31] as example) upon discharge P3-Na_xMO_2 converts to O3-Na_1MO_2, one can expect that this P3-type compound once fully

discharged should convert in a biphasic process to O3-type which obviously is not the case. To get further information, the structure evolution during the first electrochemical cycle is analyzed using *in situ* XRD.

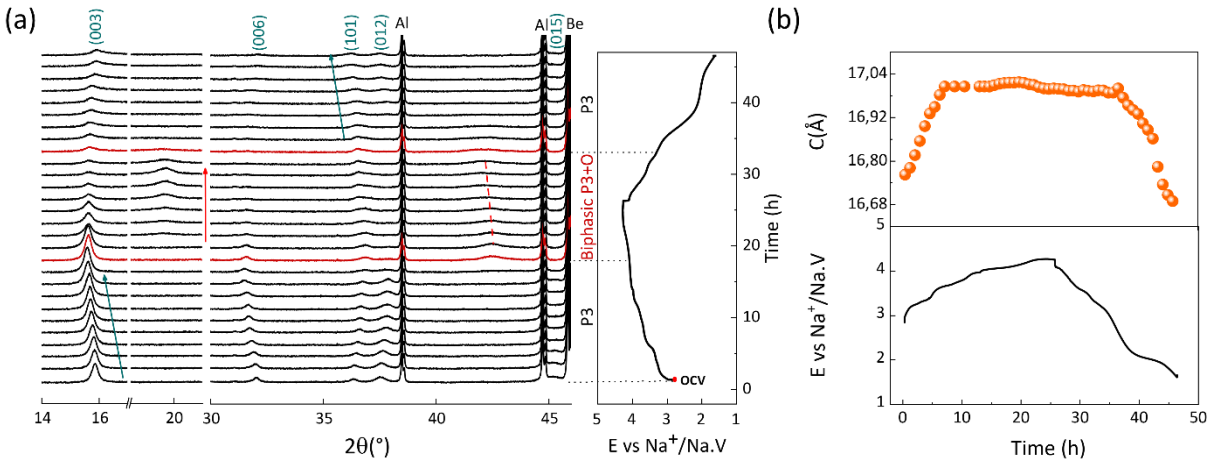

Figure 5: a) Operando XRD analysis of P3-$Na_xMn_{2/3}Ni_{1/3}O_2$ as a function of sodium deinsertion and reinsertion. The corresponding time versus voltage plot is shown on the right. b) lattice parameter variation as a function of voltage.

The evolution of the XRD patterns (Figure 5) collected during the first cycle of P3-$Na_{0.8}Mn_{2/3}Ni_{1/3}O_2$-600 shows first a shift of the Bragg peak position in agreement with a solid solution process. The extraction of Na further proceeds in three different steps starting with no clear evolution of the XRD patterns followed by the decrease in intensity of (012) peaks associated to the growth of a new peak at 2θ=42° and ending, at highest voltage, by the growth of a new peak at 2θ=21° at the expense of the Bragg peaks characteristic of the P3-type structure. Along the discharge the reverse evolution is observed indicating the reversibility of all processes. The evolution of the c cell parameter of the P3-type component confirms the initial solid solution process, the successive domains corresponding to structure conversion where no obvious cell parameter evolution is observed and their reversibility. At the end of the discharge, while P3-type structure is maintained, the c cell parameter is lower than the initial one in agreement with extra-sodiation toward stoichiometric fully discharged sample.

The evolutions observed out of the solid solution process can be interpreted in light of already reported similar evolutions for several P-type layered compounds. The evolution of the intensity of the Bragg peaks of the P3-type structure indicates intermediate structure changes corresponding to the progressive conversion from P-type to O-type structure. The process begins by the formation of P/O intergrowths followed by a clear biphasic process to form a O-type structure characterized by an abnormally short interlayer distance as indicated by the high Bragg angle observed (2θ=21°) for (00l) plane. This P-type to O-type conversion is now well-known to be rooted by the need to minimize different repulsive effects. For high Na-content, P-type is stabilized to reduce Na-Na repulsion via the zig-zag distribution in prismatic sites, while for low Na content O-type is stabilized to reduce repulsion between oxygen from adjacent MO_2 layers [26]. The strength of the effects being dependent of the Na content explains that intermediate P/O intergrowths occurs on an extended range of composition before full conversion to O-type structure.

As a summary, the exchange of Na for P3-$Na_xMn_{2/3}Ni_{1/3}O_2$ sample starts in charge by a domain of solid solution followed by the progressive conversion from P-type to O-type. These mechanisms are reversible and lead to obtain stoichiometric P-type structure at the fully discharged state but without evidence for a conversion to O-type structure. This behavior being identical to the one reported for P2-type reference compound, one can conclude that the stacking sequence P3-type does not affect the electrochemical behavior of layered oxide.

This last observation raises however another question regarding the exact nature of the high voltage and low Na content compound. More precisely, the O-type structure observed at high voltage notably the growing of a Bragg peak at 2θ=21° has been already frequently observed to appear during extraction of Na for both P2-type and O3-type compounds. Despite identical, it has been interpreted as corresponding to O2-type when obtained during desodiation of P2-type compounds and as a O-type structure without more details when obtained during

desodiation of O3-type compounds. Knowing that it is now well admitted that P-type to O-type structure conversion should maintain the stacking sequence to avoid high energy cost of breaking M-O bonds, the conversion from P2-type or P3-type structure to the same O-type structure is intriguing and shows that a deeper investigation of the actual nature of the compound obtained at high voltage is needed.

Conclusion

The investigation of the thermal behavior of mixtures between transition metal precursors and Na sources shows that the use of both transition metal and sodium hydroxide precursors is needed to solve the kinetic issues of the synthesis process and allow the synthesis at low temperature of Na_xMO_2 layered compounds whatever the main aim: synthesis of metastable polymorphs or lowering the energy cost.

The use of optimized chemical process to synthesize Na-rich P-type $Na_xMn_{1-y}Ni_yO_2$ compounds leads to stabilize, whatever the Ni content, P3-$Na_xMn_{1-y}Ni_yO_2$ layered compounds with sodium content near 0.8 far from targeted stoichiometric composition. This indicates that the use of precursor route optimized to lower the reaction temperature is not a strategy efficient enough to reach high energy density P-type compound and that maybe, other protocols to the post synthesis sodiation of stable P2-$Na_{2/3}MO_2$ have to be investigated.

In addition, the investigation of the electrochemical behavior of obtained P3-$Na_{0.8}Mn_{1-y}Ni_yO_2$ compounds shows that they behave similarly to the reference compounds indicating the absence of obvious advantage nor in preparing Na-rich P3-type homologue of stable O3-type structure neither than P3-type stacking sequence of stable P2-type homologue.

As a general conclusion, while a synthesis protocol to obtain stoichiometric P-type layered oxide has still to be designed, it is still to demonstrate that such approach will allow combining in a single active material high energy density and high power capabilities. At

least, Na-rich P3-type does not present clear advantage as they convert to O3-type upon discharge while the direct synthesis of Na-rich P2-type layered oxide remains a challenge.

Acknowledgements

This project is supported by Chimie Balard Cirimat Carnot institute through the ANR program N°16 CARN 0008-01. This research received funding from the European Union's Horizon 2020 research and innovation program under grant agreement n°875629-Naïma.

References

[1] J.B. Goodenough, Y. Kim, Challenges for rechargeable Li batteries, Chem. Mater. 22 (2010) 587–603. https://doi.org/10.1021/cm901452z.

[2] J.-M. Tarascon, M. Armand, Issues and challenges facing rechargeable lithium batteries, Nature. 414 (2001) 359–367. https://doi.org/10.1038/35104644.

[3] Y. Hu, S. Komaba, M. Forsyth, C. Johnson, T. Rojo, A New Emerging Technology: Na- Ion Batteries, Small Methods. 3 (2019) 1900184. https://doi.org/10.1002/smtd.201900184.

[4] T. Hosaka, K. Kubota, A.S. Hameed, S. Komaba, Research Development on Sodium-Ion Batteries, Chem. Rev. 120 (2020) 6358–6466. https://doi.org/10.1021/acs.chemrev.9b00463.

[5] J.Y. Hwang, S.T. Myung, Y.K. Sun, Sodium-ion batteries: Present and future, Chem. Soc. Rev. 46 (2017) 3529–3614. https://doi.org/10.1039/c6cs00776g.

[6] N. Ortiz-Vitoriano, N.E. Drewett, E. Gonzalo, T. Rojo, High performance manganese-based layered oxide cathodes: Overcoming the challenges of sodium ion batteries, Energy Environ. Sci. 10 (2017) 1051–1074. https://doi.org/10.1039/c7ee00566k.

[7] C. Delmas, C. Fouassier, P. Hagenmuller, Structural classification and properties of the layered oxides, Phys. B+C. 99 (1980) 81–85. https://doi.org/10.1016/0378-4363(80)90214-4.

[8] R. Gao, Z. Zheng, P. Wang, C. Wang, H. Ye, F. Cao, Recent advances and prospects of layered transition metal oxide cathodes for sodium-ion batteries, Energy Storage Mater. 30 (2020) 9–26. https://doi.org/10.1016/j.ensm.2020.04.040.

[9] B. Zhang, R. Dugas, G. Rousse, P. Rozier, A.M. Abakumov, J.M. Tarascon, Insertion compounds and composites made by ball milling for advanced sodium-ion batteries, Nat. Commun. 7 (2016). https://doi.org/10.1038/ncomms10308.

[10] C. Zhao, Z. Yao, Q. Wang, H. Li, J. Wang, M. Liu, S. Ganapathy, Y. Lu, J. Cabana, B. Li, X. Bai, A. Aspuru-Guzik, M. Wagemaker, L. Chen, Y.S. Hu, Revealing High Na-Content P2-Type Layered Oxides as Advanced Sodium-Ion Cathodes, J. Am. Chem. Soc. 142 (2020) 5742–5750. https://doi.org/10.1021/jacs.9b13572.

[11] H. Dong, G.M. Koenig, A review on synthesis and engineering of crystal precursors produced:

Via coprecipitation for multicomponent lithium-ion battery cathode materials, CrystEngComm. 22 (2020) 1514–1530. https://doi.org/10.1039/c9ce00679f.

[12] T. Risthaus, L. Chen, J. Wang, J. Li, D. Zhou, L. Zhang, D. Ning, X. Cao, X. Zhang, G. Schumacher, M. Winter, E. Paillard, J. Li, P3 Na0.9Ni0.5Mn0.5O2 Cathode Material for Sodium Ion Batteries, Chem. Mater. 31 (2019) 5376–5383. https://doi.org/10.1021/acs.chemmater.8b03270.

[13] S. Deng, Y. Chen, G. Kolliopoulos, V.G. Papangelakis, Y. Li, Correction to: Thermodynamic and experimental analysis of Ni-Co-Mn carbonate precursor synthesis for Li-rich cathode materials, Ionics (Kiel). 26 (2020) 4213–4213. https://doi.org/10.1007/s11581-020-03514-8.

[14] Y.J. Gu, Q.G. Zhang, Y.B. Chen, H.Q. Liu, Y.M. Wang, F.X. Hao, P. Liu, S.Q. Li, The Thermodynamic Analysis of $Ni_{1/2}Mn_{1/2}(OH)_2$ Prepared by Hydroxide Co-Precipitation Method, Adv. Mater. Res. 643 (2013) 104–107. https://doi.org/10.4028/www.scientific.net/AMR.643.104.

[15] D. Wang, I. Belharouak, L.H. Ortega, X. Zhang, R. Xu, D. Zhou, G. Zhou, K. Amine, Synthesis of high capacity cathodes for lithium-ion batteries by morphology-tailored hydroxide co-precipitation, J. Power Sources. 274 (2015) 451–457. https://doi.org/10.1016/j.jpowsour.2014.10.016.

[16] J. Lamb, A. Manthiram, Synthesis Control of Layered Oxide Cathodes for Sodium-Ion Batteries: A Necessary Step Toward Practicality, Chem. Mater. 32 (2020) 8431–8441. https://doi.org/10.1021/acs.chemmater.0c02435.

[17] P.F. Wang, H.R. Yao, X.Y. Liu, Y.X. Yin, J.N. Zhang, Y. Wen, X. Yu, L. Gu, Y.G. Guo, Na+/vacancy disordering promises high-rate Na-ion batteries, Sci. Adv. 4 (2018) 1–10. https://doi.org/10.1126/sciadv.aar6018.

[18] Q. Wang, S. Mariyappan, J. Vergnet, A.M. Abakumov, G. Rousse, F. Rabuel, M. Chakir, J. Tarascon, Reaching the Energy Density Limit of Layered O3- NaNi 0.5 Mn 0.5 O 2 Electrodes via Dual Cu and Ti Substitution, Adv. Energy Mater. 9 (2019) 1901785. https://doi.org/10.1002/aenm.201901785.

[19] J. Rodriguez-Carvajal, Recent Developments of the Program FULLPROF in Commission on Powder Diffraction (IUCr), Newsletter. 26 (2001) 12–19. https://doi.org/https://www.scirp.org/(S(i43dyn45teexjx455qlt3d2q))/reference/ReferencesPapers.aspx?ReferenceID=1479337.

[20] W. Liang, L. Li, R. Li, Y. Yin, Z. Li, X. Liu, S. Shan, Y. He, Y. Meng, Z. Li, H. Li, Crystal structure of impurity-free rhodochrosite (MnCO3) and thermal expansion properties, Phys. Chem. Miner. 47 (2020). https://doi.org/10.1007/s00269-019-01078-2.

[21] A.N. Christensen, G. Ollivier, Hydrothermal preparation and low temperature magnetic properties of Mn(OH)2, Solid State Commun. 10 (1972) 609–614. https://doi.org/10.1016/0038-1098(72)90602-3.

[22] B. Mortemard de Boisse, D. Carlier, M. Guignard, C. Delmas, Structural and Electrochemical Characterizations of P2 and New O3-Na x Mn 1-y Fe y O 2 Phases Prepared by Auto-Combustion Synthesis for Na-Ion Batteries , J. Electrochem. Soc. 160 (2013) A569–A574. https://doi.org/10.1149/2.032304jes.

[23] D.H. Lee, J. Xu, Y.S. Meng, An advanced cathode for Na-ion batteries with high rate and excellent structural stability, Phys. Chem. Chem. Phys. 15 (2013) 3304. https://doi.org/10.1039/c2cp44467d.

[24] J.M. Paulsen, R.A. Donaberger, J.R. Dahn, Layered T2-, O6-, O2-, and P2-Type

A(2/3)[M'2+(1/3)M4+(2/3)]O2 bronzes, A = Li, Na; M' = Ni, Mg; M = Mn, Ti, Chem. Mater. 12 (2000) 2257–2267. https://doi.org/10.1021/cm990810d.

[25] W. Zuo, J. Qiu, X. Liu, F. Ren, H. Liu, H. He, C. Luo, J. Li, G.F. Ortiz, H. Duan, J. Liu, M.-S. Wang, Y. Li, R. Fu, Y. Yang, The stability of P2-layered sodium transition metal oxides in ambient atmospheres, Nat. Commun. 11 (2020) 3544. https://doi.org/10.1038/s41467-020-17290-6.

[26] M.D. Radin, A. Van der Ven, Stability of Prismatic and Octahedral Coordination in Layered Oxides and Sulfides Intercalated with Alkali and Alkaline-Earth Metals, Chem. Mater. 28 (2016) 7898–7904. https://doi.org/10.1021/acs.chemmater.6b03454.

[27] M. Sathiya, J. Thomas, D. Batuk, V. Pimenta, R. Gopalan, J.M. Tarascon, Dual Stabilization and Sacrificial Effect of Na2CO3 for Increasing Capacities of Na-Ion Cells Based on P2-NaxMO2 Electrodes, Chem. Mater. 29 (2017) 5948–5956. https://doi.org/10.1021/acs.chemmater.7b01542.

[28] M. Sathiya, J. Thomas, D. Batuk, V. Pimenta, R. Gopalan, J.-M. Tarascon, Dual Stabilization and Sacrificial Effect of Na2CO3 for Increasing Capacities of Na-Ion Cells Based on P2-NaxMO2 Electrodes, Chem. Mater. 29 (2017) 5948–5956. https://doi.org/10.1021/acs.chemmater.7b01542.

[29] Z. Lu, J.R. Dahn, In Situ X-Ray Diffraction Study of P2-Na2/3[Ni1/3Mn2/3]O2, J. Electrochem. Soc. 148 (2001) A1225. https://doi.org/10.1149/1.1407247.

[30] E.J. Kim, L.A. Ma, L.C. Duda, D.M. Pickup, A. V. Chadwick, R. Younesi, J.T.S. Irvine, A.R. Armstrong, Oxygen Redox Activity through a Reductive Coupling Mechanism in the P3-Type Nickel-Doped Sodium Manganese Oxide, ACS Appl. Energy Mater. 3 (2020) 184–191. https://doi.org/10.1021/acsaem.9b02171.

[31] I. Komaba, Shinichi. Yabuuchi, Naoaki Nakayama, Tetsuri Ogata, Atsushi Ishikawa, Toru Nakai, Study on the Reversible Electrode Reaction of Na1– xNi0.5Mn0.5O2 for a Rechargeable Sodium-Ion Battery, Inorg. Chem. 51 (2012) 6211–6220. https://doi.org/10.1021/ic300357d.